*J Toxicol Pathol 2012; **25**: 27–35*

Original Article

N-Ethyl-*N*-Nitrosourea Induces Retinal Photoreceptor Damage in Adult Rats

Katsuhiko Yoshizawa[1], Tomo Sasaki[1,2], Norihisa Uehara[1], Maki Kuro[3], Ayako Kimura[1], Yuichi Kinoshita[1,4], Hisanori Miki[1], Takashi Yuri[1], and Airo Tsubura[1]

[1] Department of Pathology II, Kansai Medical University, Moriguchi, Osaka 570-8506, Japan
[2] Kyoto R & D Center, Maruho Co., Ltd., Kyoto, Kyoto 600-8815, Japan
[3] Department of Ophthalmology, Kansai Medical University, Moriguchi, Osaka 570-8507, Japan
[4] Department of Cytopathology, Kansai Medical University Takii Hospital, Moriguchi, Osaka 570-8507, Japan

Abstract: Seven-week-old male Lewis rats received a single intraperitoneal injection of *N*-ethyl-*N*-nitrosourea (ENU) (100, 200, 400 or 600 mg/kg), and retinal damage was evaluated 7 days after the treatment. Sequential morphological features of the retina and retinal DNA damage, as determined by a TUNEL assay and phospho-histone H2A.X (γ-H2AX), were analyzed 3, 6, 12, 24 and 72 hr, 7 days, and/or 30 days after 400 mg/kg ENU treatment. Activation of the nuclear enzyme poly (ADP-ribose) polymerase (PARP) was analyzed immunohistochemically by poly (ADP-ribose) (PAR) expression in response to DNA damage of the retina. All rats that received ≥ 400 mg/kg of ENU developed retinal degeneration characterized by the loss of photoreceptor cells in both the central and peripheral retina within 7 days. In the 400 mg/kg ENU-treated rats, TUNEL-positive signals were only located in the photoreceptor cells and peaked 24 hr after ENU treatment. The γ-H2AX signals in inner retinal cells appeared at 24 hr and peaked at 72 hr after ENU treatment, and the PAR signals selectively located in the photoreceptor cell nuclei appeared at 12 hr and peaked at 24 hr after ENU treatment. However, degeneration was restricted to photoreceptor cells, and no degenerative changes in inner retinal cells were seen at any time points. Retinal thickness and the photoreceptor cell ratio in the central and peripheral retina were significantly decreased, and the retinal damage ratio was significantly increased 7 days after ENU treatment. In conclusion, ENU induced retinal degeneration in adult rats that was characterized by photoreceptor cell apoptosis through PARP activity. (DOI: 10.1293/tox.25.27; J Toxicol Pathol 2012; 25: 27–35)

Key words: *N*-ethyl-*N*-nitrosourea, γ-H2A.X, PAR, PARP, photoreceptor cell, retinal degeneration, rat

Introduction

N-Ethyl-*N*-nitrosourea (ENU) is an alkylating agent that is particularly effective in inducing congenital malformations[1,2] and tumors of systemic organs including the nervous tissue in rodents[3]. ENU mutagenesis has been used to create a large number of random point mutations in the genomic DNA of mice and zebrafish and is a powerful tool for creating animal models of disease[4,5], such as morphological defects in the eyes[6,7] and retinal degeneration in the progeny of treated animals[8–10]. A single intraperitoneal injection of ENU also induces retinal and corneal damage in mature mice[11,12]; however, the mechanism of ENU-induced retinal damage in adult rodents is unclear.

Double-strand breaks (DSBs), the most deleterious kind of alteration to DNA, are produced by exogenous agents. One of the earliest events in the DNA damage response is the Ser139 phosphorylation of histone H2A.X (γ-H2AX), which is a critical factor for cellular protection against DNA alkylating agents[13–16]. DNA alkylating agents also activate poly (ADP-ribose) polymerase (PARP)[17]. In several retinal damage models, such as NMDA-induced ganglion cell loss[18], retinal ischemia/reperfusion injury[19], retinal degeneration 1 (rd1) mice carrying the *Pde 6b* gene[20], and *N*-methyl-*N*-nitrosourea (MNU)-induced photoreceptor apoptosis[21], cell death is linked to PARP hyperactivation.

The purpose of this research is to evaluate the effect of ENU on the retinal cells of adult rats and to focus on the activation of γ-H2AX and PARP as DNA damage responses in the retina after ENU exposure.

Materials and Methods

Animals

Fifty-two male Lewis rats [LEW/CrlCrlj] obtained from Charles River Laboratories Japan (Osaka, Japan) were

Received: 1 September 2011, Accepted: 31 October 2011
Mailing address: Katsuhiko Yoshizawa, Department of Pathology II, Kansai Medical University, 10-15 Fumizono, Moriguchi, Osaka 570-8506, Japan
TEL: 81-6-6993-9431 FAX: 81-6-6992-5023
E-mail: yoshizak@takii.kmu.ac.jp

used at 7 weeks of age. Rats were maintained in specific pathogen-free conditions and received free access to a commercial diet (CMF 30Gy; Oriental Yeast, Chiba, Japan) and tap water. The animals were housed in plastic cages with paper-chip bedding (Paper Clean, SLC, Hamamatsu, Japan) in an air-conditioned room at 22 ± 2 °C and 60 ± 10% relative humidity with a 12-hr light/dark cycle. The illumination intensity was less than 60 lux in the cages. All procedures were in accordance with the guidelines for animal experimentation at Kansai Medical University.

Chemical and dose formulation

ENU (*N*-Nitroso-*N*-ethylurea bulk package®; chemical formula, $C_3H_7N_3O_2$) was purchased from Sigma-Aldrich Japan (Tokyo, Japan) and kept at −80 °C in the dark. It was dissolved in physiologic saline just prior to use.

Experimental procedures

The experiments consisted of 2 independent studies, the purpose being to confirm the dose dependency of the retinal lesions in the 1st study and to confirm the sequential changes in the 2nd study. Sixteen rats received an intraperitoneal (ip) injection of ENU at a dose of 100, 200, 400 or 600 mg/kg (4 rats/group). Seven days after injection, rats were anesthetized with isoflurane (Forane®, Abbott Japan, Tokyo, Japan) and sacrificed by exsanguination from abdominal aortic transection. In another experiment, 28 rats received a single ip injection of 400 mg/kg of ENU, and 4 randomly selected mice were sacrificed at 7 time points (3, 6, 12, 24 and 72 hr and 7 and 30 days) after treatment. In each experiment, the control groups consisted of 4 rats that were treated with vehicle (physiological saline) only. All rats were observed daily for clinical signs of toxicity and were weighed at the time of ENU treatment and on the day of sacrifice. Both eyes were quickly removed at the time of sacrifice, and complete necropsies were conducted on all animals.

Tissue fixation and processing

One eye from each rat was fixed overnight in 10% neutral buffered formalin, and the other eye was fixed overnight in methacarn (60% methanol, 30% chloroform and 10% acetic acid). Subsequently, the eyes were embedded in paraffin, sectioned at a thickness of 4 μm, and stained with hematoxylin and eosin (HE). Ocular sections were cut along a line parallel to the optic axis and nerve (including the ora serrata). Histologic and morphometric evaluations were performed by a toxicologic pathologist certified by the Japanese Society of Toxicologic Pathology and the International Academy of Toxicologic Pathology (K.Y.) and an ophthalmologist certified by the Japanese Ophthalmological Society (M.K.), according to the previously defined histopathological terminology and diagnostic criteria[11,22].

Morphometric analysis of retinal thickness, photoreceptor cell ratio and retinal damage ratio

HE-stained sections of the retina were scanned with a high-resolution digital slide scanner (NanoZoomer 2.2 Digital Pathology, Hamamatsu Photonics, Hamamatsu, Japan) to prepare digital images. The ndpi image files were opened in color mode with the NDP.view software (Hamamatsu Photonics). The total retinal thickness (from the internal limiting membrane to the pigment epithelium), inner retinal thickness (from the internal limiting membrane to the outer plexiform layer) and outer retinal thickness (from the outer nuclear layer to the pigment epithelial cell layer) were individually measured from methacarn-fixed HE slides using NDP.view, as described in our previous reports[11,22]. The measurements were conducted at the central retina (approximately 400 μm from the optic nerve) and peripheral retina (approximately 400 μm from both sides of the ciliary bodies). To further evaluate the photoreceptor cell loss, the photoreceptor ratio [(outer retinal thickness / total retinal thickness) × 100] was calculated. To determine the area of retinal damage, the entire length of the retina and the length of the damaged area in HE preparations were measured. Damaged retina was designated as the presence of less than four rows of photoreceptor nuclei in the outer nuclear layer[11,22], and the retinal damage ratio was calculated as: (length of damaged retina / whole retinal length) × 100.

TUNEL, phospho-histone H2A.X, and poly (ADP-ribose) immunohistochemistry

Formalin-fixed eye sections at 6 time points (3, 6, 12, 24 and 72 hr and 7 days) after treatment with 400 mg/kg ENU and at 7 days after vehicle treatment were used for the analyses of cell death and DNA damage responses. Cell death was observed by terminal deoxynucleotidyl transferase (TdT)-mediated dUTP digoxigenin nick end-labeling (TUNEL) using an in situ apoptosis detection kit (ApopTag; Millipore, Bellerica, MA, USA) according to previous reports[11,22]. Sequential sections were immunohistochemically stained with anti-phospho-histone H2A.X (γ-H2AX) monoclonal antibody (Ser139, 1:200 in dilution; Cell Signaling Technology, Danvers, MA, USA), an immunomarker of the DNA damage response[14,16,23] and anti-poly (ADP-ribose) (PAR) monoclonal antibody (10H, 1:200 in dilution; Enzo Life Sciences International, Plymouth Meeting, PA, USA), an immunomarker of the activation of poly (ADP-ribose) polymerase (PARP)[19–21]. PAR is synthesized after the activation of the nuclear DNA repair enzyme PARP. Antigen retrieval was necessary for γ-H2AX visualization and was conducted by pressure-cooker heating (Pascal, Dako, Carpinteria, CA, USA). Each primary antibody was reacted overnight under 4 °C, and the antigen–antibody complexes were identified using an LSAB staining kit (Dako) according to the manufacturer's instructions. The reaction products were visualized with 3–3′-diaminobenzidine tetrahydrochloride.

Apoptotic and γ-H2AX cell ratio and PAR immunoreactivity

TUNEL- and γ-H2AX-stained retinal sections were scanned with a high-resolution digital slide scanner to prepare digital images. The images were captured at 40 × magnification. The apoptotic cell ratio was calculated from TU-

NEL-stained slides by determining the number of apoptotic nuclei of photoreceptor cells per microscopic field at the central retina and peripheral retina. The γ-H2AX-positive cells were counted in three microscopic fields per whole retina in a random fashion. The intensity grade of immune staining and expression for PAR in the retina was scored as negative, weak, moderate or strong.

Statistical analysis

All discrete values, expressed as means ± standard error (SE), were analyzed using the two-tailed independent Student's *t*-test for unpaired samples after confirming the homogeneity of variances. The results presented below include comparisons between ENU-treated mice and vehicle-treated mice. P values < 0.05 were considered to show statistical significance.

Results

General remarks

Mortality and body weight of ENU-treated rats were affected in a dose-dependent manner. Rats treated with 600 mg/kg ENU exhibited decreased locomotor activity, and 2 of the 4 rats in this group died on day 7. There was a statistically significant decrease in the growth rates (weight gain) in all ENU-treated groups; the growth rates were 61%, 92%, 115%, 120% and 127% in the 600, 400, 200 and 100 mg/kg groups and the control group, respectively. The growth rate of the 400 mg/kg ENU-treated group decreased at 24 hr, peaked at day 7, and recovered at day 30 (data not shown).

Morphological and morphometric analysis of dose-dependent retinal damage

The results of histological evaluation of the retinas of ENU- and vehicle-treated rats were compared 7 days after ENU treatment. The retinas of control rats contained more than 10 layers of photoreceptor nuclei in the central retina and more than 8 layers of cells in the peripheral retina (Fig. 1). All rats treated with 600 mg/kg ENU had either no photoreceptor cell nuclei or only a few rows of photoreceptor cell nuclei, such that the outer nuclear layer and photoreceptor layer almost disappeared in both the central and peripheral retina (Fig. 1). In 400 mg/kg ENU-treated rats, the central retina contained no photoreceptor cell nuclei or only a few rows of photoreceptor cell nuclei (Fig. 1), and the peripheral retina contained 5 or fewer rows of photoreceptor cell nuclei. The remaining photoreceptor nuclei were densely stained and contained clumped chromatin, suggesting that they were degenerating. The ENU-induced changes were restricted to photoreceptor cells; all other layers of the retina remained intact 7 days after ENU treatment. No other ENU-induced changes to the components of the eye (including the cornea) were observed. The retinas of all rats that received 200 mg/kg ENU or less were histopathologically intact (Fig. 1).

Seven days after treatment with 600 mg/kg ENU, the total retinal thickness and outer retinal thickness were significantly decreased in both the central and peripheral retina, as compared with the control rats (Fig. 1), whereas 400 mg/kg ENU caused a decrease in thickness in only the central retina with statistical significance (Fig. 2a). Changes in the inner retinal thickness were not observed in any of the ENU-treated groups (data not shown). To further evaluate the ENU-induced effects on retinal thickness, the photoreceptor cell ratio was calculated (Fig. 2a). The photoreceptor cell ratios at the central and peripheral retinas were 43% and 51% for control rats, but only 10% and 11% ($P<0.01$) in the 600 mg/kg ENU-treated rats and 9% ($P<0.01$) and 43% (not significant) in the 400 mg/kg ENU-treated rats. The photoreceptor cell ratios at the central and peripheral retina were not significantly different in rats treated with 200 mg/kg ENU or less (46% and 50% in the 200 mg/kg group and 46% and 50% in the 100 mg/kg group, respectively). To evaluate the degree of disease progression, the retinal damage ratio was compared among the groups (Fig. 2b). The 600 and 400 mg/kg ENU-induced damages were 100% and 56%, respectively, while the damage was 0% in the 200 and 100 mg/kg ENU-treated groups and vehicle-treated rats.

Morphological and morphometric analyses of sequential changes in retinal damage

Six hours after treatment with 400 mg/kg ENU, condensation and fragmentation of photoreceptor cell nuclei and vacuolar change in the photoreceptor layer occurred. The disruption and loss of the photoreceptor cell nuclei progressed at 24 hr, and widespread destruction and disappearance of photoreceptor segments occurred at 72 hr (Fig. 3). A majority of the photoreceptor cell nuclei were lost in the central retina at day 7. As a result, the thickness of the total retina and the outer retina of ENU-treated rats decreased progressively, and cystoid degeneration was seen in the inner retinal layer 30 days after treatment (Fig. 3). The photoreceptor cell ratio at the central and peripheral retina was decreased significantly from 24 hr after ENU treatment; the photoreceptor cell ratios in the central and peripheral retina were decreased by 39% and 45% at 24 hr, 28% and 40% at 72 hr, and 9% and 44% at day 7, respectively, and by 43% and 51% in control rats (Fig. 4). The retinal thickness on day 30 was similar to the thickness 7 days after treatment. During the disease course, no inflammatory cell infiltration was seen in the retina.

Apoptotic cell ratio

In both the central and peripheral retina of the 400 mg/kg ENU-treated rats, the TUNEL signal appeared selectively in the photoreceptor cell nuclei, and some pyknotic photoreceptor cell nuclei at 6 and 12 hr showed TUNEL positivity without obvious nuclear destruction. Many photoreceptor cell nuclei showed TUNEL positivity at 24 hr after treatment (Fig. 5a). The sequential changes in the apoptotic cell ratio at 0, 3, 6, 12, 24 and 72 hr and 7 days were 0.6, 0.5, 2.8, 13.4, 44.5, 19.8 and 1.4, respectively, in the central retina and 0.1, 0.1, 2.4, 15.5, 46.3, 21.1 and 0.6, respectively, in the peripheral retina (Fig. 5b).

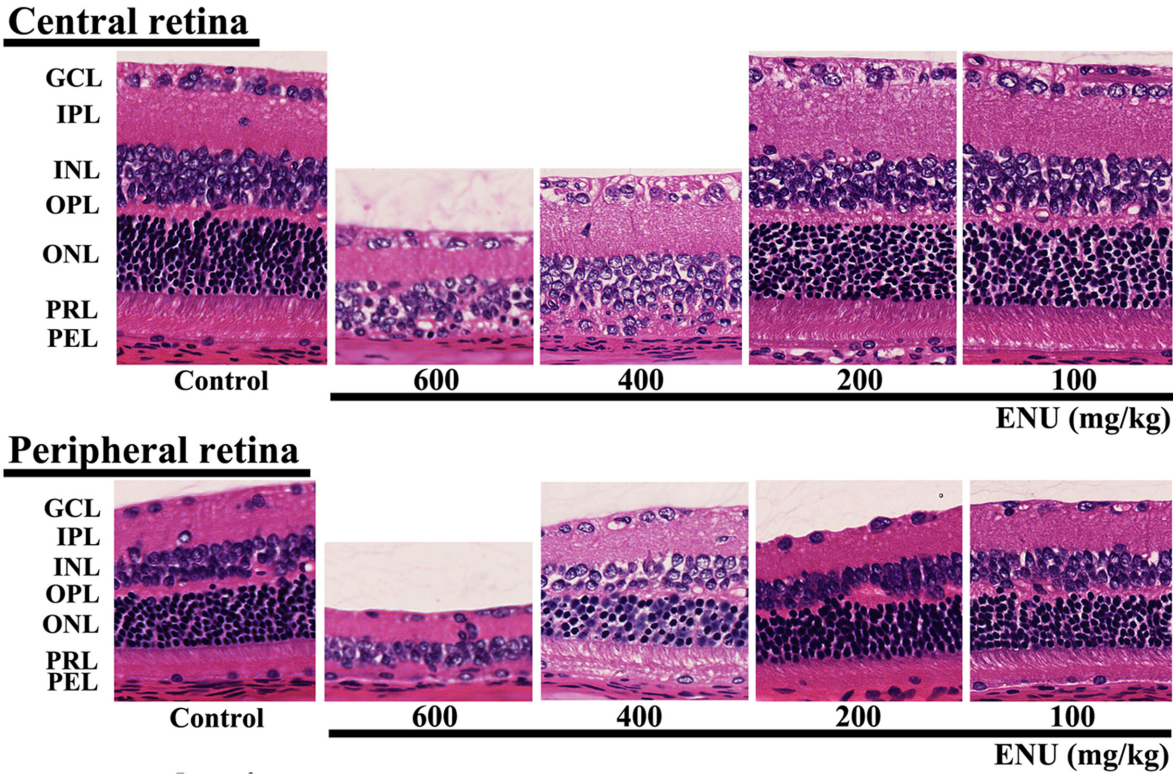

Fig. 1. Retinal change in adult rats 7 days after a single ip injection of ENU. The outer nuclear layer and photoreceptor layer degenerated and/or disappeared in both the peripheral and central retina of rats who received ≥ 400 mg/kg ENU. No change was seen in the retinas of rats treated with 200 or 100 mg/kg ENU. GCL, ganglion cell layer; IPL, inner plexiform layer; INL, inner nuclear layer; OPL, outer plexiform layer; ONL, outer nuclear layer; PRL, photoreceptor layer; and PEL, pigment epithelial layer. HE staining, ×400.

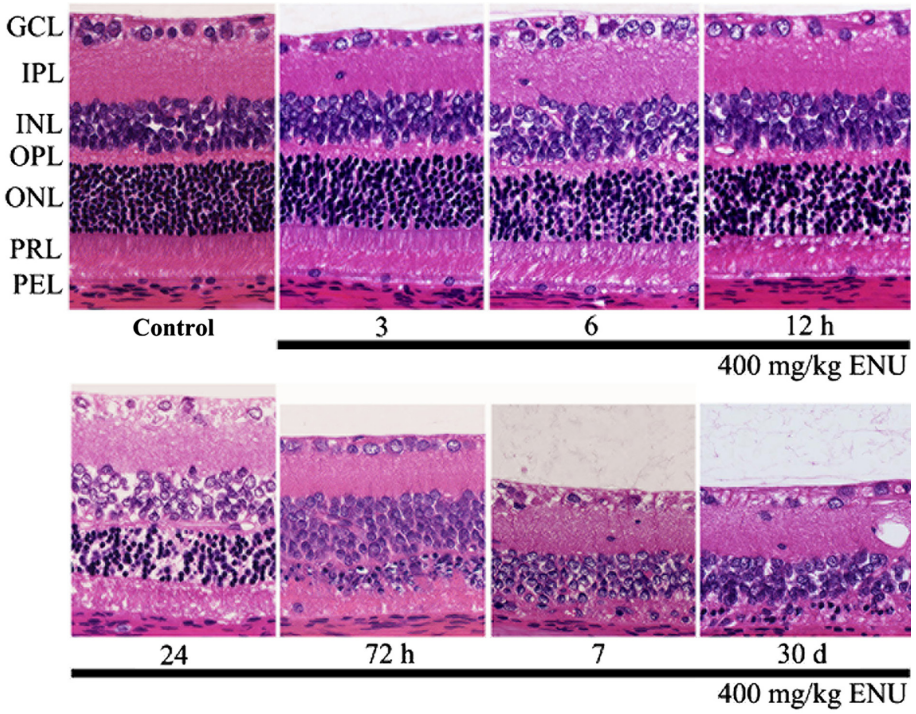

Fig. 3. Sequential retinal changes in adult rats after a single ip injection of 400 mg/kg ENU. Retinal cross sections were collected 3, 6, 12, 24 and 72 hr and 7 and 30 days after ENU treatment. GCL, ganglion cell layer; IPL, inner plexiform layer; INL, inner nuclear layer; OPL, outer plexiform layer; ONL, outer nuclear layer; PRL, photoreceptor layer; and PEL, pigment epithelial layer. HE staining, ×400.

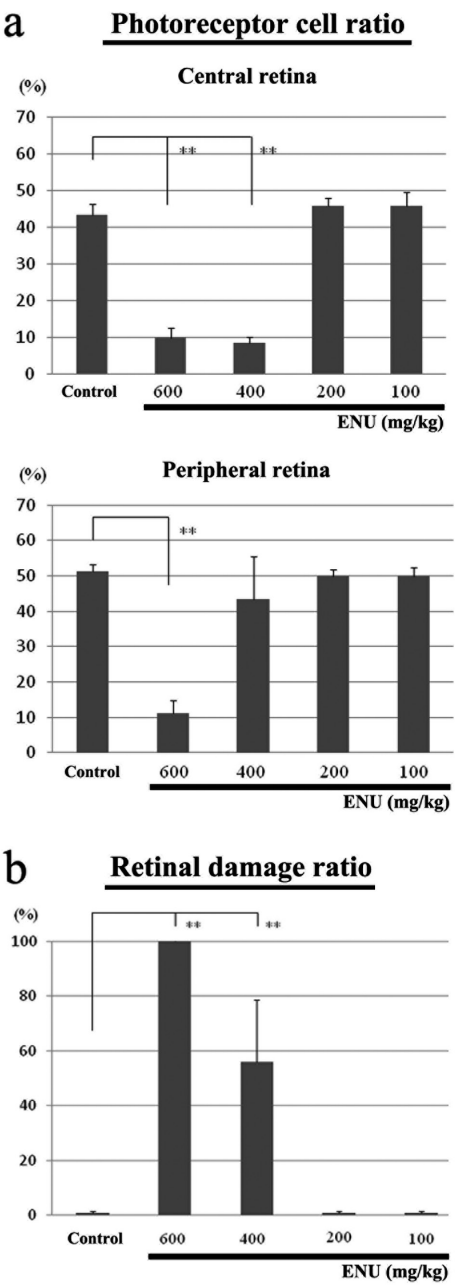

Fig. 2. Photoreceptor cell ratios in the central retina and peripheral retina 7 days after a single ip injection of ENU into adult rats (a). Rats treated with 600 and 400 mg/kg ENU had a statistically significant decrease in photoreceptor ratio at the central and/or peripheral retina, as compared with saline-treated controls. The index was calculated as [(outer retinal thickness/total retinal thickness) × 100]. Retinal damage ratios in ENU-treated adult rats (b). The index was evaluated as [(length of retina composed of less than four rows of photoreceptor cells/whole retinal length) × 100]. The mean ± SE of the four rats in each treatment group is shown. **: P<0.01.

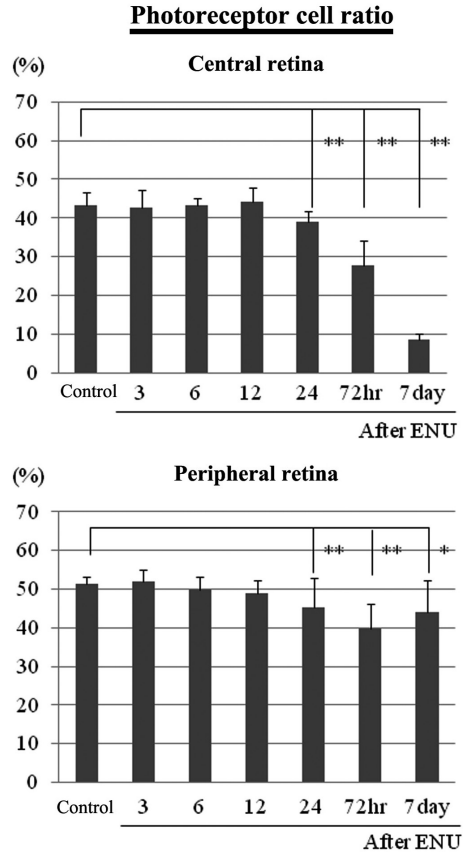

Fig. 4. Sequential changes in the photoreceptor cell ratios of the central and peripheral retina after a single ip injection of 400 mg/kg ENU into adult rats. The index was calculated as [(outer retinal thickness/total retinal thickness) × 100]. The mean ± SE of the four rats in each treatment group is shown. * and **: P<0.05 and P<0.01, respectively.

γ-H2AX cell ratio and PAR immunoreactivity

In the retinas of the 400 mg/kg ENU-treated rats, the γ-H2AX-positive cells were scattered almost evenly in the the whole retina. The γ-H2AX signal was localized to the the cell nuclei in the inner nuclear layer and was not accompanied by any obvious morphological nuclear changes. The signal appeared 24 hr after ENU treatment, and the index peaked 72 hr after ENU treatment (Fig. 6a). The sequential changes in the γ-H2AX cell ratio were 0, 0, 0, 0, 3, 16.3 and 1.8 at 0, 3, 6, 12, 24 and 72 hr and 7 days (Fig. 6b). PAR signals were not detected in the control retina. At 12 hr after ENU treatment, the signals were localized to the photoreceptor cell nuclei at the central and peripheral retina. The expression peaked at 24 hr after treatment, and the signals disappeared 7 days after treatment.

Discussion

The present study provides new evidence of ENU-induced retinal changes. Retinal degeneration characterized by the loss of the outer nuclear layer and photoreceptor layer in the central and peripheral retina was detected in ENU-treated adult rats after a single ip injection of ≥ 400 mg/kg ENU. The outer nuclear layer and photoreceptor layer of ENU-treated rats decreased progressively due to photoreceptor cell apoptosis, which was characterized by the pres-

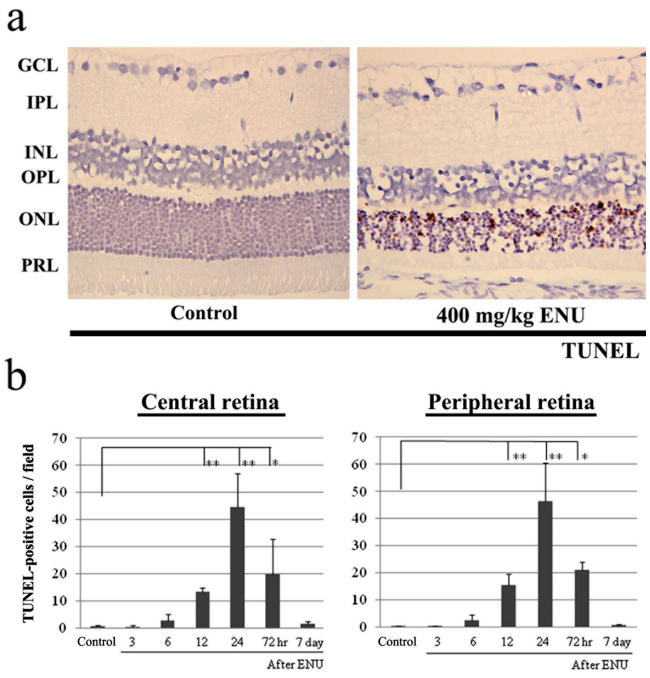

Fig. 5. TUNEL-positive photoreceptor cells in the outer nuclear layer 24 hr after a single ip injection of 400 mg/kg ENU into adult rats (a). The signals are seen in many photoreceptor cell nuclei, although no or few signals are seen in the control retina (b). GCL, ganglion cell layer; IPL, inner plexiform layer; INL, inner nuclear layer; OPL, outer plexiform layer; ONL, outer nuclear layer; PRL, photoreceptor layer; and PEL, pigment epithelial layer. TUNEL staining, ×400. Sequential changes in the apoptotic cells per field were evaluated in the central and peripheral retina, respectively (c). Mean ± SE; each bar represents four rats. * and **: P<0.05 and P<0.01, respectively.

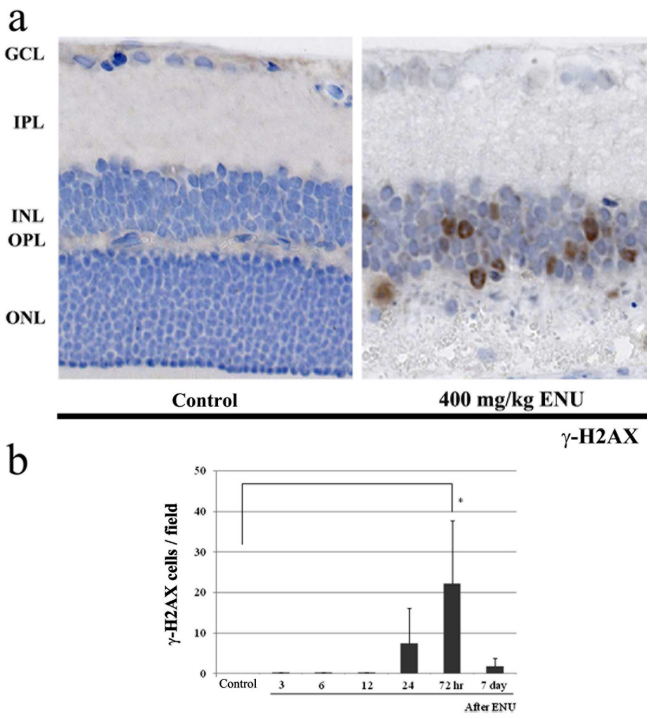

Fig. 6. γ-H2AX-positive cells per field in the inner nuclear layer 72 hr after a single ip injection of 400 mg/kg ENU into adult rats (a). The signals are seen in several inner retinal cell nuclei, although no signals are seen in the control retina (b). GCL, ganglion cell layer; IPL, inner plexiform layer; INL, inner nuclear layer; OPL, outer plexiform layer; and ONL, outer nuclear layer. γ-H2AX immunohistochemical staining, ×800. Sequential changes in the γ-H2AX-positive cells of the inner retina (c). Mean ± SE, each bar represents four rats. * and **: P<0.05 and P<0.01, respectively.

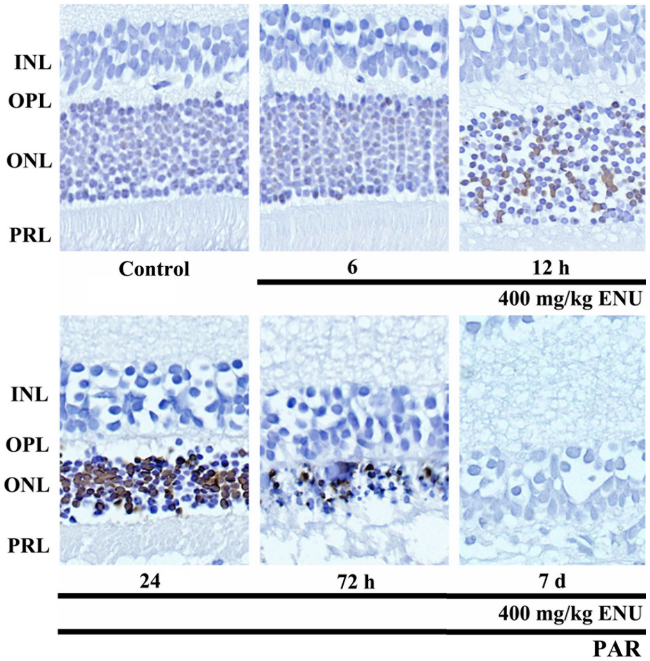

ence of TUNEL-positive nuclei restricted to photoreceptor cells. Photoreceptor cell apoptosis was evident at 6 hr and peaked at 72 hr after ENU treatment, followed by extensive photoreceptor cell loss at day 7. A morphometric analysis showed that photoreceptor cell damage occurred similarly in both the central and peripheral retina in rats treated with 600 mg/kg ENU, while 400 mg/kg ENU caused loss of outer retinal layers located mainly in the central retina at 7 days after exposure. Therefore, the central retina may be more sensitive to ENU-induced damage. ENU is a stem-cell mutagen that also affects hematopoietic stem cells and immune cells, and animals are highly susceptible to infection after injection of ENU[24]. In the present study, the deaths in the 600 mg/kg dose group may have been caused by hematopoietic toxicity and immunotoxicity.

Fig. 7. Sequential PAR expression in the retina after a single ip injection of 400 mg/kg ENU into adult rats. PAR immunoreactivities located in the photoreceptor cell nuclei were seen at 12 hr and peaked at 24 hr after ENU treatment. INL, inner nuclear layer; OPL, outer plexiform layer; ONL, outer nuclear layer; and PRL, photoreceptor layer. PAR immunohistochemical staining, ×600.

ENU is the most potent mutagen in rodents[4,5,25], and it can be used to generate point mutations throughout the mouse genome[25]. Various mouse models for human diseases have been generated by a systematic, large-scale, genome-wide phenotyping screen in the last decade[5]. The eyes of ENU-treated animals exhibit morphological defects, such as lens opacity, microphthalmia, corneal adhesion, corneal opacity, pink eye, iris anomalies, coloboma, and preretinal blood vessels[5–7]. The progeny of ENU-treated animals exhibit retinal degeneration[8–10]. In addition, a single ip injection of 100 mg/kg ENU on day 14 of gestation or of 200 mg/kg ENU on day 3 after birth induces rosette-like structures (dysplasia) in the retinas of fetal and neonatal rats, respectively[2,26]. Although ENU has been used as a carcinogen and mutagen in many animal toxicity and carcinogenesis studies, there has been only one report concerning the effect of ENU on the retinas of adult mice[11], and this previous study was conducted by our group. To the best of our knowledge, the present study is the first report on ENU-induced retinal injury in adult rats.

Inherited night blindness is a fairly widespread disease in humans, and it affects approximately one in 5,000 individuals worldwide. A common form of inherited blindness is retinitis pigmentosa, which is a degenerative pigmentary retinopathy that is noninflammatory, bilateral and progressive[27,28]. Animal models of retinal degeneration are important for elucidating the mechanism of human retinitis pigmentosa[28–30] and exploring potential treatments[28,31]. The retinal degeneration (photoreceptor cells loss) induced by *N*-methyl-*N*-nitrosourea (MNU), which is an ENU-related compound[25], has been well studied as one of the rodent models of retinitis pigmentosa[22,31]. MNU causes DNA adduct formation in photoreceptor nuclei, followed by apoptosis via the downregulation of Bcl-2, upregulation of Bax and activation of the PARP and caspase families in rats. In contrast, few studies have focused on ENU-induced retinal damage in adult rodents.

In the present study, ENU induced an increased number of TUNEL-positive photoreceptor cells in parallel with the expression of PAR signals. The PAR signals were expressed selectively in the photoreceptor cell nuclei. The signals appeared 12 hr after ENU treatment, and the immunoreactivity peaked 72 hr after ENU treatment. PAR is synthesized after activation of the nuclear DNA repair enzyme PARP. However, under conditions of severe DNA damage, excessive activation of PARP results in depletion of the cellular pool of nicotinamide adenine dinucleotide and ATP, which is followed by cell death[21].

γ-H2AX is a critical factor for cellular protection against DNA alkylating agents[15], and it can mediate DNA repair[13,14,16,32]. Methylating agents such as MNU can cause cell-cycle arrest, γ-H2AX expression and cell death, either via caspase-dependent apoptosis or via a PARP-dependent form of apoptosis[33]. Two forms of γ-H2AX expression have been elucidated. The transient form of γ-H2AX expression is associated with the repair and removal of double-strand breaks from the nucleus. The other form of γ-H2AX expression involves the formation of foci by more persistent double-strand breaks that tend to accumulate and remain unrepaired in cells[14]. In ENU-induced retinal damage, γ-H2AX signals appeared in the inner retinal cells 24 hr after ENU exposure, peaked at 72 hr and then disappeared. No cell death in the inner retina could be seen at any point, suggesting that the cells recovered from the DNA damage. The identity of the γ-H2AX-positive cells located in the inner nuclear layer (bipolar cells, horizontal cells, amacrine cells or Muller cells) was not determined. Moreover, γ-H2AX expression was not detected in the outer retina where cell death occurred. Further studies concerning the DNA damage cascade and cell type in the inner retina are necessary to understand the detailed pathogenesis of ENU-induced γ-H2AX expression in the inner retina.

Hypofluorescence in indocyanine green angiography is seen in the chorioretinal atrophic area in MNU-treated retinal degeneration[34]. Also, the vascular sequential changes in MNU-treated retinal degeneration have been reported[35]; the numbers of acellular capillaries, ghost cells and vessels exhibiting narrowing in trypsin-digested retinal vessels were increased after MNU exposure. These data may suggest ischemic or hypoxic conditions in the retina after MNU exposure. Under ischemic or hypoxic conditions, target cells express γ-H2AX as a DNA damage response and progress through the DNA repair pathway[36]. In our study, although angiographic analysis was not conducted, the inner retina may have been under ischemic or hypoxic conditions after ENU exposure, and this may have been followed by progression through the DNA repair pathway. Therefore, γ-H2AX expression in the inner retina may be a secondary effect due to the ischemic or hypoxic conditions that developed after the outer retinal damage was induced by ENU exposure.

The survival of neurons from the potentially damaging events caused by unregulated cell-protective signaling and DNA repair is a complex process that requires multiple steps and enzymes. Exposure to ENU causes the formation of DNA adducts, such as O^6-alkylguanine, in the target cells[37–39]. The adduct is removed by repair enzymes such as O^6-methylguanine-DNA methyltransferase (MGMT)[38,40]. Additionally, DNA polymerase β is essential for the repair of DNA lesions damaged by exogenous genotoxin[41]. DNA polymerase β is responsible for 99% of the polymerase activity in neurons[42] and is upregulated during light-induced retinal degeneration[43]. Further studies of the DNA repair cascade in the inner retina are necessary to understand the detailed pathogenesis of ENU-induced retinal degeneration.

In conclusion, retinal degeneration occurred in adult rats after a single intraperitoneal injection of 400 mg/kg ENU. ENU-induced retinal degeneration was related to photoreceptor cell apoptosis via PARP activation. The γ-H2AX signals were expressed only in inner retinal cells and disappeared promptly, suggesting that the inner retinal cells recovered from DNA damage. Investigations of the detailed mechanisms of ENU-induced retinal degeneration are necessary for a better understanding of the pathogenesis of chemical-induced retinal degeneration.

Acknowledgements: The authors thank Ms. T. Akamatsu for her technical assistance and Ms. A. Shudo for preparing the manuscript. The authors declare that they have no competing financial interests. This research was supported in part by a Grant-in Aid for Scientific Research (C) from the Japan Society for the Promotion of Science (22591954).

References

1. Diwan BA. Strain-dependent teratogenic effects of 1-ethyl-1-nitrosourea in inbred strains of mice. Cancer Res. **34**: 151–157. 1974. [Medline]
2. Nagaishi T. Effects of ethylnitrosourea on the developing rat retina. Nippon Ganka Gakkai Zasshi. **86**: 1224–1235. 1982 (Abstract in English, text in Japanese). [Medline]
3. World Health Organization, International Agency for Research on Cancer (WHO IARC). *N*-nitroso-*N*-ethylurea. In: IARC Monographs on the Evaluation of Carcinogenic Risks to Humans, Vol. 17, Some N-Nitroso Compounds, IARC Scientific Publications, Lyon, France. 191. 1998.
4. Probst FJ, and Justice MJ. Mouse mutagenesis with the chemical supermutagen ENU. Methods Enzymol. **477**: 297–312. 2010. [Medline] [CrossRef]
5. Wagner S, Calzada-Wack J, Rosemann M, Becher L, Tost M, Silva-Buttkus P, Klein-Rodewald T, Fuchs H, Neff F, Hrabe de Angelis M, and Esposito I. Characterization of ENU-mutant mice. Animal models for human diseases using morphological and molecular methods. Pathologe. (Suppl 2): 147–152. 2010 (Abstract in English, text in German). [Medline] [CrossRef]
6. Baird PN, Guymer RH, Chiu D, Vincent AL, Alexander WS, Foote SJ, and Hilton DJ. Generating mouse models of retinal disease using ENU mutagenesis. Vis Res. **42**: 479–485. 2002. [Medline] [CrossRef]
7. Favor J, and Neuhauser-Klaus A. Saturation mutagenesis for dominant eye morphological defects in the mouse *Mus musculus*. Mamm Genome. **11**: 520–525. 2000. [Medline] [CrossRef]
8. Maaswinkel H, Mason B, and Li L. ENU-induced late-onset night blindness associated with rod photoreceptor cell degeneration in zebrafish. Mech Ageing Dev. **124**: 1065–1071. 2003. [Medline] [CrossRef]
9. Liu H, Wang M, Xia CH, Du X, Flannery JG, Ridge KD, Beutler B, and Gong X. Severe retinal degeneration caused by a novel rhodopsin mutation. Invest Ophthalmol Vis Sci. **51**: 1059–1065. 2010. [Medline] [CrossRef]
10. Sato H, Suzuki T, Ikeda K, Masuya H, Sezutsu H, Kaneda H, Kobayashi K, Miura I, Kurihara Y, Yokokura S, Nishida K, Tamai M, Gondo Y, Noda T, and Wakana S. A monogenic dominant mutation in Rom1 generated by *N*-ethyl-*N*-nitrosourea mutagenesis causes retinal degeneration in mice. Mol Vis. **16**: 378–391. 2010. [Medline]
11. Yoshizawa K, Kuro-Kuwata M, Sasaki T, Lai C, Kanematsu S, Miki H, Kimura-Kawanaka A, Uehara N, Yuri T, and Tsubura A. Retinal degeneration induced in adult mice by a single intraperitoneal injection of *N*-ethyl-*N*-nitrosourea. Toxicol Pathol. **39**: 606–613. 2011. [Medline] [CrossRef]
12. Yoshizawa K, Sasaki T, Kuro M, Miki H, Kimura A, Uehara N, Yuri T, and Tsubura A. Corneal damage induced in adult mice by a single intraperitoneal injection of *N*-ethyl-*N*-nitrosourea. In Vivo. **25**: 609–615. 2011. [Medline]
13. Mah LJ, El-Osta A, and Karagiannis TC. γ-H2AX: a sensitive molecular marker of DNA damage and repair. Leukemia. **24**: 679–686. 2010. [Medline] [CrossRef]
14. Mah LJ, El-Osta A, and Karagiannis TC. γ-H2AX as a molecular marker of aging and disease. Epigenetics. **5**: 129–136. 2010. [Medline] [CrossRef]
15. Meador JA, Zhao M, Su Y, Narayan G, Geard CR, and Balajee AS. Histone H2AX is a critical factor for cellular protection against DNA alkylating agents. Oncogene. **27**: 5662–5671. 2008. [Medline] [CrossRef]
16. Redon CE, Nakamura AJ, Zhang YW, Ji J, Bonner WM, Kinders RJ, Parchment RE, Doroshow JH, and Pommier Y. Histone γH2AX and poly(ADP-ribose) as clinical pharmacodynamic biomarkers. Clin Cancer Res. **16**: 4532–4542. 2010. [Medline] [CrossRef]
17. Burkle A. Poly(ADP-ribosyl)ation, a DNA damage-driven protein modification and regulation of genomic instability. Cancer Lett. **163**: 1–5. 2001. [Medline] [CrossRef]
18. Goebel DJ, and Winkler BS. Blockade of PARP activity attenuates poly(ADP-ribosyl)ation but offers only partial neuroprotection against NMDA-induced cell death in the rat retina. J Neurochem. **98**: 1732–1745. 2006. [Medline] [CrossRef]
19. Li SY, Yang D, Yeung CM, Yu WY, Chang RC, So KF, Wong D, and Lo AC. Lycium barbarum polysaccharides reduce neuronal damage, blood-retinal barrier disruption and oxidative stress in retinal ischemia/reperfusion injury. PLoS ONE. **6**: e16380. 2011. [Medline] [CrossRef]
20. Paquet-Durand F, Silva J, Talukdar T, Johnson LE, Azadi S, Van Veen T, Ueffing M, Hauck SM, and Ekstrom PAR. Excessive activation of poly(ADP-ribose) polymerase contributes to inherited photoreceptor degeneration in the retinal degeneration 1 mouse. J Neurosci. **27**: 10311–10319. 2007. [Medline] [CrossRef]
21. Uehara N, Miki K, Tsukamoto R, Matsuoka Y, and Tsubura A. Nicotinamide blocks *N*-methyl-*N*-nitrosourea-induced photoreceptor call apoptosis in rats through poly (ADP-ribose) polymerase activity and Jun N-terminal kinase/activator protein-1 pathway inhibition. Exp Eye Res. **82**: 488–495. 2006. [Medline] [CrossRef]
22. Yoshizawa K, Nambu H, Yang J, Oishi Y, Senzaki H, Shikata N, Miki H, and Tsubura A. Mechanisms of photoreceptor cell apoptosis induced by *N*-methyl-*N*-nitrosourea in Sprague-Dawley rats. Lab Invest. **79**: 1359–1367. 1999. [Medline]
23. Baleriola J, Suarez T, and De la Rosa EJ. DNA-PK promotes the survival of young neurons in the embryonic mouse retina. Cell Death Differ. **17**: 1697–1706. 2010. [Medline] [CrossRef]
24. Justice MJ, Carpenter DA, Favor J, Neuhauser-Klaus A, Harbe de Angelis M, Soewarto D, Moser A, Cordes S, Miller D, Chapman V, Weber JS, Rinchik EM, Hunsicker PR, Rissell WL, and Bode VC. Effects of ENU dosage on mouse strains. Mamm Genome. **11**: 484–488. 2000. [Medline] [CrossRef]
25. Gnewuch CT, and Sosnovsky G. A critical appraisal of the evolution of *N*-nitrosourea as anticancer drugs. Chem Rev. **97**: 829–1014. 1997. [Medline] [CrossRef]
26. Maeda H, Matsuo T, Nagaishi T, and Ikeda T. Supraependymal cell clusters induced by ENU treatment in developing rat retina. Cong Anom. **25**: 129–135. 1985.
27. Hartong DT, Berson EL, and Dryja TP. Retinitis pigmen-

tosa. Lancet. **368**: 1795–1809. 2006. [Medline] [CrossRef]
28. Shintani K, Shechtman DL, and Gurwood AS. Review and update: current treatment trends for patients with retinitis pigmentosa. Optometry. **80**: 384–401. 2009. [Medline] [CrossRef]
29. Rivas MA, and Vecino E. Animal models and different therapies for treatment of retinitis pigmentosa. Histol Histopathol. **24**: 1295–1322. 2009. [Medline]
30. Sancho-Pelluz J, Arango-Gonzalez B, Kustermann S, Romero FJ, van Veen T, Zrenner E, Ekström P, and Paquet-Durand F. Photoreceptor cell death mechanisms in inherited retinal degeneration. Mol Neurobiol. **38**: 253–269. 2008. [Medline] [CrossRef]
31. Tsubura A, Yoshizawa K, Kuwata M, and Uehara N. Animal models for retinitis pigmentosa induced by MNU; disease progression, mechanisms and therapeutic trials. Histol Histopathol. **25**: 933–944. 2010. [Medline]
32. Kuo LJ, and Yang LX. γ-H2AX- a novel biomarker for DNA double-strand breaks. In Vivo. **22**: 305–309. 2008. [Medline]
33. McDaid JR, Loughery J, Dunne P, Boyer JC, Downes CS, Farber RA, and Walsh CP. MLH1 mediates PARP-dependent cell death in response to the methylating agent *N*-methyl-*N*-nitrosourea. Br J Cancer. **101**: 441–451. 2009. [Medline] [CrossRef]
34. Nagai Y, Matsubara T, Takahashi K, Nakajima M, Nambu H, Tsubura A, and Uyama M. Angiographic findings and histological localization of indocyanine green in *N*-methyl-*N*-nitrosourea induced retinal degeneration in rats. Nihon Ganka Gakkai Zasshi **103**: 489–496. 1999; (Abstract in English, text in Japanese). [Medline]
35. Nakatani A, Matsuura T, Ozaki K, and Narama I. Microangiopathy associated with MNU-induced retinal degeneration in mice. J Toxicol Pathol. **23:** M10. 2010 (Abstract from The 26th Annual Meeting of The Japanese Society of Toxicologic Pathology).
36. Olcina M, Lecane PS, and Hammond EM. Targeting hypoxic cells through the DNA damage response. Clin Cancer Res. **16**: 5624–5629. 2010. [Medline] [CrossRef]
37. Thomale J, Huh NH, Nehls P, Eberle G, and Rajewsky MF. Repair of O^6-ethylguanine in DNA protects rat 208F cells from tumorigenic conversion by *N*-ethyl-*N*-nitrosourea. Proc Natl Acad Sci USA. **87**: 9883–9887. 1990. [Medline] [CrossRef]
38. Tosal L, Comendador MA, and Sierra LM. *In vivo* repair of ENU-induced oxygen alkylation damage by the nucleotide excision repair mechanism in *Drosophila melanogaster*. Mol Genet Genomics. **265**: 327–335. 2001. [Medline]
39. Pegg AE. Mammalian O^6-alkylguanine-DNA alkyltransferase: regulation and importance in response to alkylating carcinogenic and therapeutic agents. Cancer Res. **50**: 6119–6129. 1990. [Medline]
40. Ishikawa T, Zhang SS, Qin X, Takahashi Y, Oda H, Nakatsuru Y, and Ide F. DNA repair and cancer: lessons from mutant mouse models. Cancer Sci. **95**: 112–117. 2004. [Medline] [CrossRef]
41. Yoshizawa K, Jelezcova E, Brown AR, Foley JF, Nyska A, Cui X, Hofseth LJ, Maronpot RM, Wilson SH, Sepulveda AR, and Sobol RW. Gastrointestinal hyperplasia with altered expression of DNA polymerase β. PLoS ONE. **4**: Article number e6493. 2009. [Medline] [CrossRef]
42. Waser J, Hubscher U, Knenzle CC, and Spadari S. DNA polymerase B from brain neurons is a repair enzyme. Eur J Biochem. **97**: 361–368. 1979. [Medline] [CrossRef]
43. Cortina MS, Gordon WC, Lukiw WJ, and Bazan NG. DNA repair in photoreceptor survival. Mol Neurobiol. **28**: 111–122. 2003. [Medline] [CrossRef]